European Conference on Optical Communication (ECOC) 2022 © Optica Publishing Group 2022

All-optical any-to-any wavelength conversion across 36nm range

Aneesh Sobhanan[(1)], Vladimir Gordienko[(1)], Chandra B Gaur[(1,2)], Andrew Ellis[(1*)]

[(1)] Aston Institute of Photonic Technologies, Aston University, Birmingham, B4 7ET, UK
[(2)] Now with SubCom LLC, 250 Industrial Way W, Eatontown, NJ 07724, USA
*andrew.ellis@aston.ac.uk

Abstract *We experimentally demonstrate all-optical wavelength conversion with efficiency above -5 dB from any wavelength to any other wavelength across a whole of the C band by employing two narrow-linewidth pumps in Al-doped HNLF. ©2022 The Author(s)*

Introduction

Wavelength conversion especially conversion from an arbitrary wavelength to a desired wavelength over a broad-bandwidth is essential to optimize the network cost and efficiency. It provides increase in reach of multi-band optical networks[1]. A Raman-assisted wavelength conversion over broad band was shown in[2],[3] with conversion efficiency greater than 0 dB in HNLF. A 80 nm arbitrary wavelength conversion using partially degenerate pump in ZD-DS HNLF was presented in[4]. Flexible wavelength conversion using dispersion flattened fibers were reported before[4],[5]. However, such fiber has low nonlinear coefficient, which adversely affects the conversion efficiency. A two-stage cascaded FWM in low-dispersion slope HNLF was used for arbitrary wavelength conversion over 30 nm[6] and a guard-band-less and polarization-insensitive tunable wavelength conversion[7]. Thus wisely selecting the pump wavelength in the zero dispersion wavelength (λ_{ZD}) of the highly nonlinear fiber (HNLF) to satisfy the phase-matching condition among the signal, idler and pump waves[8] or using two-stage cascaded FWM using HNLF[6] were in general used for efficient conversion. In all these demonstrations the flexibility of all-optical wavelength conversion is limited by the tunability of the pump wavelength with respect to the signal and idler wavelengths around the λ_{ZD}.

Another limiting factor in standard HNLF is stimulated Brillouin scattering (SBS) which sets an upper limit in the amount of pump power which can be launched[8]. The maximum conversion efficiency which can be achieved in silica fibers without SBS mitigation is below -10dB[9]. Phase dithering of the pump is one of the methods to increase the SBS threshold[10]. However, phase dithering is not a good choice for many of the applications. Applying strain gradient along the length of the fiber[11] is another method to increase the SBS threshold. But, straining the fiber can reduce the fiber life time and also it inflicts a large dispersion variation and thus significantly reduces operation bandwidth[12]. Recently, aluminium doping in the core of HNLF was proved to be the best choice to suppress the SBS and such a fiber with reduced loss was presented in[13]. Aluminium doping raises the refractive index and lowers the acoustic index and thus hindering the SBS to build up. Such Al- doped fibers were used in phase regeneration using FWM based PSAs and in generation of high repetition rate short-pulses[14],[15].

In this work we use two pumps to double the total pump power without inducing SBS and thus significantly improve conversion efficiency (above -5 dB) using an Al-doped HNLF. A combination of wavelength shifts and phase conjugations enables any-to-any wavelength conversion across 36nm range (within the range 1535.5 to 1571.5nm) whilst adjusting pump wavelengths within 20nm range. Also, this scheme requires only a single FWM-stage without any guard bands due to flexibility enabled by employing two pumps.

Principle and Experimental setup

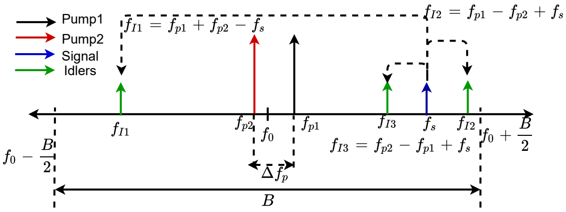

Fig. 1: Schematic of any-to-any wavelength conversion with in a signal bandwidth of B

One of the key challenges to enable any-to-any wavelength conversion is to facilitate pump amplification across the required pump wavelength tuning range. Operation of high power EDFAs required for pump amplification is typically limited to ~20nm wavelength range. Therefore, we have developed a novel concept to allow any-

European Conference on Optical Communication (ECOC) 2022 © Optica Publishing Group 2022

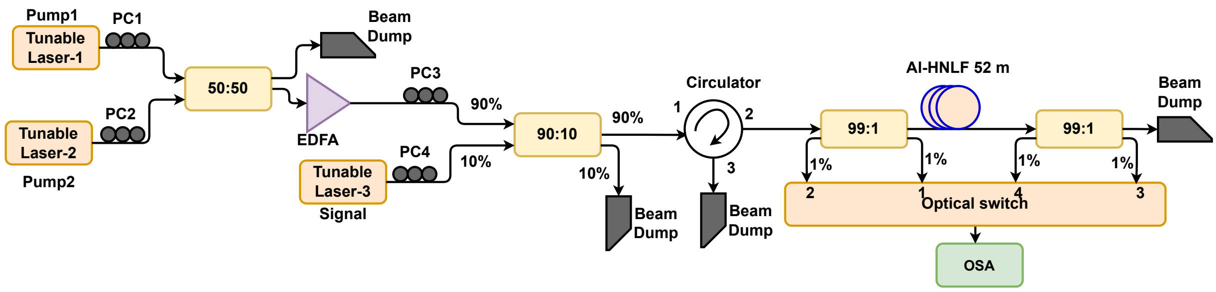

Fig. 2: Experimental setup to measure SBS and conversion efficiency of AOWC

to-any wavelength conversion across the signal bandwidth B, whilst restricting the required pump wavelength range tunability to the bandwidth of $B/2$.

The idea is to employ one of two types of wavelength conversion depending on the required wavelength conversion. One type is the phase conjugating wavelength conversion where the output signal frequency is symmetric with the input signal frequency around the average frequency of pumps (f_{I1} at Fig. 1), which only requires a single sign reversal in the coherent receiver to correct for its phase conjugation[16]. Another type is frequency shift where the output signal frequency is different from the input signal frequency by the difference between the pump frequencies (f_{I2} and f_{I3} at Fig. 1). Then, any translation of signal frequency by up to $B/2$ can be performed by frequency shifts facilitated by two pumps which frequencies are adjusted within a range of $B/2$. Any translation by more than $B/2$ can be performed by phase conjugating wavelength conversion where average central frequency of the two pumps is adjusted within the range $[B/4; 3B/4]$ which is again $B/2$ wide.

We perform an experiment to verify this concept and measure conversion efficiencies for both phase conjugating and frequency shifting copies of wavelength conversions. According to our proposal it is possible to perform any-to-any wavelength conversion of the signal across the whole of C band (1528-1568nm) by adjusting pump's wavelengths within the range 1538-1558nm. Although high-power EDFAs operating across such a range can be sourced, the high power EDFA available to us had operation wavelength range of 1546-1566nm. Therefore, we set the lowest available pump wavelength of 1546nm (represented by black arrow in Fig. 1, near to the center frequency f_0 of the signal band). Other pump is then scan over the range of 1547-1566nm (red arrow in Fig. 1) in step of 1nm to get the required wavelength conversion combinations with in the signal-band.

Fig. 2 shows the experimental setup for an arbitrary wavelength converter. The setup contains two tunable laser sources (TLS) for two pumps which are combined using a 3 dB coupler to amplify using a high power EDFA to provide enough pump power required for efficient wavelength conversion. Another TLS which is tunable in the wavelength range of interest (1525.5-1571.5 nm) is used as signal source and is coupled with the pump sources through 90:10 coupler. The polarization controllers (PCs) are used to align the polarization of the laser sources so that the nonlinear mixing happens efficiently inside HNLF. These combined three waves through the 90% port of the coupler are fed to the Al-doped HNLF through a circulator. A 52 m Al-doped HNLF, with insertion loss less than 1 dB, nonlinear co-efficient γ of 8.8 $W^{-1}km^{-1}$, low dispersion slope of 0.024 $ps/nm^2/km$ and with λ_{ZD} around 1543nm, is used as the converting nonlinear medium. An optical switch and OSA are used to monitor the input (switch port-1), output (port3) and reflected power (port 2) from the HNLF via a calibrated set of 1% tap couplers.

Results and discussion

A pump-power of 34 dBm each and a signal power of 3.6 dBm are used in the wavelength converter stage, while the back-scattered power is measured to be 35 dB down with respect to pump power. This ensures that the pump powers used are well below the SBS-threshold of the HNLF. The idlers considered here are f_{I1},the conjugates and f_{I2}& f_{I3} the frequency shifted copies to accomplish any-to-any wavelength conversion in the entire signal bandwidth B as discussed in Fig 1. We calculate conversion efficiency (η) as a ratio between the output idler and the input signal powers corrected for the pump ASE noise: $\eta = \frac{P_{I_o} - P_{N_o}}{P_{S_{in}} - P_{N_{in}}}$, where, P_{N_o}-the pump ASE noise in the output idler, P_{I_o}-output idler power, $P_{N_{in}}$-the signal in-band noise and the $P_{S_{in}}$-input signal power at corresponding wavelengths.

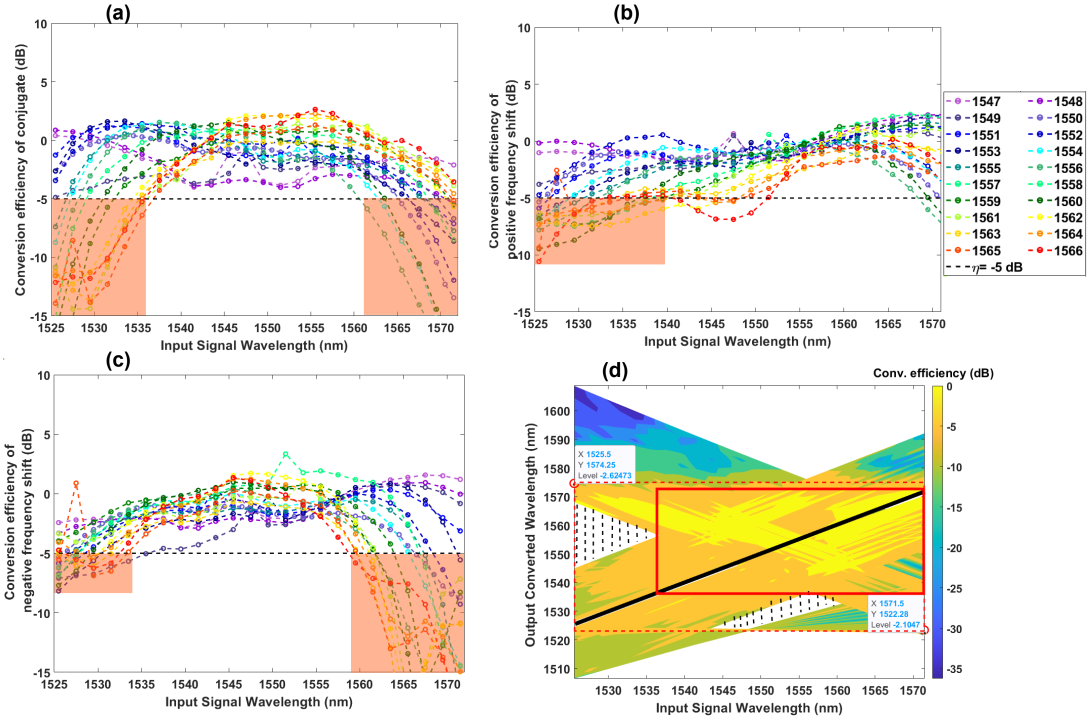

Fig. 3: Idler conversion efficiency vs. signal wavelength: λ_{p1}=1546 nm and λ_{p2} tuned with in 20 nm with respect to λ_{p1} ($< B/2$ detuning) (a) I_1, (b) I_2, (c) I_3, The dotted black line: $\eta = -5dB$. The line color is coded such that the color varies from Indigo to Red in the order of increasing pump2 wavelength, (d) contour plot showing any-to-any wavelength conversion

Fig. 3(a)-(c), shows the conversion efficiencies of three idlers, f_{I1}, f_{I2} and f_{I3} as a function of signal wavelength for different λ_{p2} . It can be seen that most of the converted idlers are generated with efficiency above -5 dB (those with $\eta < -5$ dB are shown in the shaded region). When the pump2 is at 1566 nm (maximum detuning) and if the signal is in the bandwidth edge (say 1525.5 or 1571.5nm in this experiment), idlers f_{I2} or f_{I3} at 1505.5 to 1591.5nm are generated, but are outside of the signal band.

To analyse the results further, we do a contour-plot as shown in Fig. 3(d), where x-axis is the signal wavelength λ_s, y-axis the idler wavelength λ_i and z-axis the corresponding efficiencies (η). A red-dotted box is marked where the points out-side of which are mostly with low efficiency and are corresponding to the shaded region in Fig. 3(a)-(c). Any-to-any conversion achieved over 36 nm (1535.5-1571.5nm) is shown inside the red-solid box. Also, we can see that most of the examined area inside the red-solid box is covered by at least one idler with conversion efficiency over -5 dB. The narrow diagonal black-strip can be neglected as it represents same to same wavelength conversion where "conversion is not needed". It is reasonable to note that the longest conversion from 1525.5nm to 1574nm and from 1571.5 to 1522nm (marked in the red circle in the diagonal corners of the red dot-box) generated with conversion efficiency above -3 dB. The white-strips with black-dotted lines indicate the area where it was not possible to examine as it requires phase-conjugating conversions with pumps central frequency below 1546nm, which is outside of the EDFA operation range. However, those intermediate conversion potentially can be filled by tuning pump1 wavelength below 1546nm near to the λ_{ZD} with a customized EDFA supporting those wavelength range which can further increase the wavelength conversion bandwidth.

In summary, we demonstrate a novel concept to enable broadband any-to-any wavelength conversion employing two pumps, Al-doped HNLF and two types of wavelength conversions. This has allowed to achieve the full flexibility of input and output signal wavelengths across a wide band, whilst tuning pump wavelength across only half of this range. We have achieved conversion efficiency >-5 dB for any-to-any wavelength conversion across a 36nm range. This configuration can enable a practical all-optical any-to-any wavelength conversion in modern C-band communication systems.

Acknowledgements

We thank the following fundings: EP/S003436/1 PHOS and Huawei Technologies (Contract number: YBN2020025011). The data underlying this publication can be found at: `https://doi.org/10.17036/researchdata.aston.ac.uk.00000546`

References

[1] H. Kawahara, M. Nakagawa, T. Seki, and T. Miyamura, “Experimental demonstration of wavelength-selective band/direction-switchable multi-band oxc using an inter-band all-optical wavelength converter”, in *ECOC*, 2020, pp. 1–4.

[2] M. Tang, Y. Gong, and P. Shum, “Broad-band tunable wavelength conversion using raman-assisted parametric four-wave mixing in highly nonlinear fibers with double-pass geometry”, *IEEE Photonics Technology Letters*, vol. 17, no. 1, pp. 148–150, 2005.

[3] V. Gordienko, M. Stephens, F. Ferreira, and N. Doran, “Raman-amplified pump and its use for parametric amplification and phase conjugation”, *Optical Fiber Technology*, vol. 56, p. 102 183, 2020.

[4] M. Takahashi, K. Mukasa, and T. Yagi, “Full c-l band tunable wavelength conversion by zero dispersion and zero dispersion slope hnlf”, in *ECOC*, 2009, pp. 1–2.

[5] K. Saitoh and M. Koshiba, “Highly nonlinear dispersion-flattened photonic crystal fibers for supercontinuum generation in a telecommunication window”, *Opt. Express*, vol. 12, no. 10, pp. 2027–2032, May 2004.

[6] S. Petit, T. Kurosu, M. Takahashi, T. Yagi, and S. Namiki, “Low penalty uniformly tunable wavelength conversion without spectral inversion over 30 nm using sbs-suppressed low-dispersion-slope highly nonlinear fibers”, *IEEE Photonics Technology Letters*, vol. 23, no. 9, pp. 546–548, 2011.

[7] T. Inoue, K. Tanizawa, and S. Namiki, “Guard-band-less and polarization-insensitive tunable wavelength converter for phase-modulated signals: Demonstration and signal quality analyses”, *Journal of Lightwave Technology*, vol. 32, no. 10, pp. 1981–1990, 2014.

[8] M. E. Marhic, *Fiber Optical Parametric Amplifiers, Oscillators and Related Devices*. Cambridge University Press, 2007.

[9] V. Gordienko, Ã. Szabo, M. Stephens, V. Vassiliev, C. Gaur, and N. Doran, “Limits of broadband fiber optic parametric devices due to stimulated brillouin scattering”, *Optical Fiber Technology*, vol. 66, p. 102 646, 2021.

[10] J. B. Coles, B. P.-P. Kuo, N. Alic, *et al.*, “Bandwidth-efficient phase modulation techniques for stimulated brillouin scattering suppression in fiber optic parametric amplifiers”, *Opt. Express*, vol. 18, no. 17, pp. 18 138–18 150, Aug. 2010.

[11] J. M. C. Boggio, J. D. Marconi, and H. L. Fragnito, “Experimental and numerical investigation of the sbs-threshold increase in an optical fiber by applying strain distributions”, *J. Lightwave Technol.*, vol. 23, no. 11, p. 3808, Nov. 2005.

[12] C. Lundstrom, R. Malik, L. Gruner-Nielsen, *et al.*, “Fiber optic parametric amplifier with 10-db net gain without pump dithering”, *IEEE Photonics Technology Letters*, vol. 25, no. 3, pp. 234–237, 2013.

[13] L. Grüner-Nielsen, D. Jakobsen, S. Herstrøm, *et al.*, “Brillouin suppressed highly nonlinear fibers”, in *ECOC*, Optica Publishing Group, 2012, We.1.F.1.

[14] R. Slavík, F. Parmigiani, J. Kakande, *et al.*, “All-optical phase and amplitude regenerator for next-generation telecommunications systems”, *Nature Photonics*, vol. 4, no. 10, pp. 690–695, 2010.

[15] R. Slavik, F. Parmigiani, L. Gruner-Nielsen, *et al.*, “Stable and efficient generation of high repetition rate ($>$ 160 ghz) subpicosecond optical pulses”, *IEEE Photonics Technology Letters*, vol. 23, no. 9, pp. 540–542, 2011.

[16] A. A. I. Ali, M. Tan, M. A. Z. Al-Khateeb, C. Laperle, and A. D. Ellis, “First demonstration of optical phase conjugation with real time commercial transceiver”, in *ECOC*, 2019, pp. 1–4.